Wide wavelength range tunable one-dimensional silicon nitride nano-grating guided mode resonance filter based on azimuthal rotation

doi: 10.1063/1.4975344

Wide wavelength range tunable one-dimensional silicon nitride nano-grating guided mode resonance filter based on azimuthal rotation

Cite as: AIP Advances **7**, 015313 (2017); https://doi.org/10.1063/1.4975344
Submitted: 12 September 2016 . Accepted: 20 January 2017 . Published Online: 30 January 2017

Ryoji Yukino, Pankaj K. Sahoo, Jaiyam Sharma, Tsukasa Takamura, Joby Joseph, and Adarsh Sandhu

Wide wavelength range tunable one-dimensional silicon nitride nano-grating guided mode resonance filter based on azimuthal rotation

Ryoji Yukino,[1] Pankaj K. Sahoo,[2] Jaiyam Sharma,[3] Tsukasa Takamura,[4] Joby Joseph,[2] and Adarsh Sandhu[1,a]

[1]*Graduate School of Information and Engineering, University of Electro-Communications, Tokyo 182-8585, Japan*

[2]*Photonics Research Lab, Department of Physics, Indian Institute of Technology Delhi, New Delhi 110016, India*

[3]*Department of Electrical and Electronic Information Engineering, Toyohashi University of Technology, Toyohashi 441-8580, Japan*

[4]*Electronics Inspired Interdisciplinary Research Institute, Toyohashi University of Technology, Toyohashi 441-8580, Japan*

(Received 12 September 2016; accepted 20 January 2017; published online 30 January 2017)

We describe wavelength tuning in a one dimensional (1D) silicon nitride nano-grating guided mode resonance (GMR) structure under conical mounting configuration of the device. When the GMR structure is rotated about the axis perpendicular to the surface of the device (azimuthal rotation) for light incident at oblique angles, the conditions for resonance are different than for conventional GMR structures under classical mounting. These resonance conditions enable tuning of the GMR peak position over a wide range of wavelengths. We experimental demonstrate tuning over a range of 375 nm between 500 nm~875 nm. We present a theoretical model to explain the resonance conditions observed in our experiments and predict the peak positions with show excellent agreement with experiments. Our method for tuning wavelengths is simpler and more efficient than conventional procedures that employ variations in the design parameters of structures or conical mounting of two-dimensional (2D) GMR structures and enables a single 1D GMR device to function as a high efficiency wavelength filter over a wide range of wavelengths. We expect tunable filters based on this technique to be applicable in a wide range of fields including astronomy and biomedical imaging. [http://dx.doi.org/10.1063/1.4975344]

When light incident on a sub-wavelength grating is allowed to couple into an underlying waveguide, the scattered light shows strong resonance over a narrow range of wavelengths. This type of optical scattering is known as guided mode resonance (GMR) and such devices have important applications as optical wavelength filters in displays,[1] image sensors,[2,3] and biosensors.[4–7] Filters based on GMR structures are important due to their narrow bandwidth and high efficiency.[8–10] In conventional devices, the GMR peak wavelength is tuned by either changing the structural parameters of devices[8,11] or by externally tuning the angle of incidence (θ) light onto the device.[10] However, the experimental set-up for theta rotation necessitates the use of a compensator mirror[10] to move synchronously with the GMR device thereby enabling consistent detection across all incident angles of light. In practice, it is difficult to integrate compensating mirrors into real-world devices. An optimized tunable filter using nematic liquid crystals has been reported by Abdulhalim.[12] Microelectromechanical systems (MEMS) methods have also been used to tune the GMR wavelength by changing the GMR structure parameters.[13–15]

[a]Electronic mail: sandhu@uec.ac.jp

GMR structures are generally operated in the so called 'classical mounting' configuration where the plane of incidence of light and the grating vector are parallel to each other. In contrast to the classical mounting, conical mounting, where the grating vector is not parallel to the plane of incidence has been shown to have applications such as in producing polarization independent output from GMR structures.[16] However, only special cases of conical mounting have been reported in literature where, for example, the plane of incidence is rotated by 90^o from the grating vector, known as full conical mounting.[16–19] In a case of general conical mounting, Szeghalmi et. al.[20] reported that the output peak wavelength from a 2D GMR nanostructure could be tuned by rotating the device azimuthally about the axis normal to the substrate. They achieved a wavelength tuning range of 150 nm with a maximum reflection efficiency of less than 20% by rotating a shallow polycarbonate nanostructure. The cause of wavelength tuning was explained as being via an apparent change in periodicity of the nanostructure on azimuthal rotation.

Here, we take this approach further and show that wavelength tuning in a 1D GMR structure can be achieved by azimuthally rotating it about the surface normal. In contrast to the 2D nanostructure described above, our 1D structure reported here was readily fabricated using well established thin film evaporation and lithography processes, yielded wider wavelength tuning range, and higher GMR peak efficiency. Moreover, we show that an apparent change in periodicity does not explain wavelength tuning in a 1D structure. Rather, tuning is explained by a change in the propagation constant of the light wave coupled from the grating into the waveguide which changes the GMR resonance condition. We expect that the above principle would better explain wavelength tuning in 2D GMR structures rather than the apparent change in periodicity.

The optical response of GMR structures strongly depends on the angle of incidence of the illuminating light. When the GMR structure is rotated azimuthally about an axis perpendicular to the surface normal, the diffracted orders get deviated from the plane of incidence and lie on the surface of a cone. This is called conical diffraction by a grating. In our experiments, we found that conical diffraction gives rise to optical filtering in a 1D GMR structure which can be tuned by its azimuthal rotation. The general conical diffraction problem for a 1D grating is described in Refs. 21–22. The properties of GMR structures under conical mounting such as resonance conditions, resonance wavelength tuning, and efficiency of GMR peak are different from classical mounting as described below.

Consider a GMR structure that is a 1D grating on a planar waveguide on a substrate as shown in Fig. 1(a). The 1D grating shown has a grating vector **K** along the x-axis with a magnitude $2\pi/\Lambda$, where

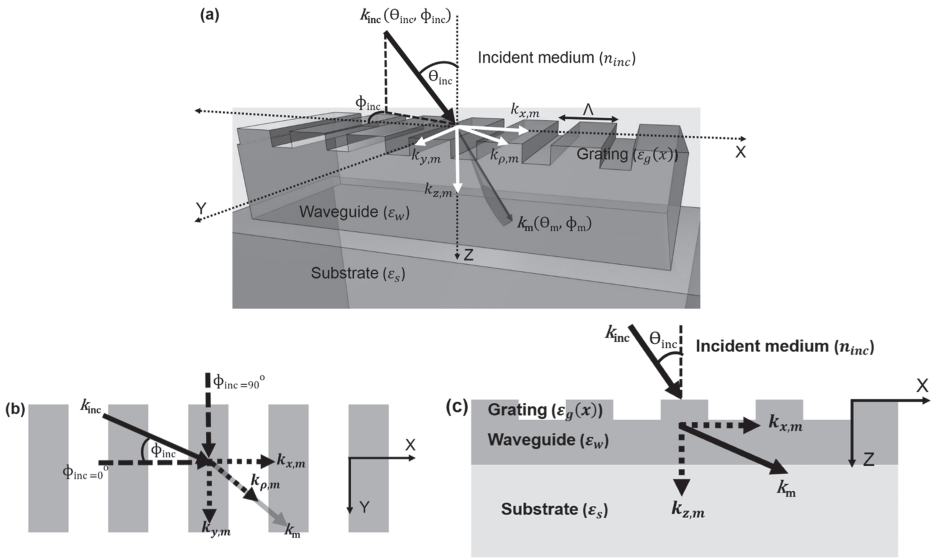

FIG. 1. Schematic of conical diffraction from GMR structure (a) complete 3D view showing the diffracted components of incident wave vector (b) Top view of (a), and (c) Cross sectional view of (a).

Λ is the grating period. The average dielectric constant of the grating region is ϵ_{avg}. The incident wave vector ($\boldsymbol{k}_{inc}$) in the incidence medium (n_{inc}) is denoted by a set of two spherical coordinate angles (θ_{inc} & ϕ_{inc}). θ_{inc} is the angle between the incident light beam and the normal (Z-axis) to the grating surface, whereas ϕ_{inc} is the angle between the plane of incidence with respect to the X-axis. Under azimuthal rotation, the x,y,z- components of the incident wave vector, $\mathbf{k}_{inc}$ can be expressed in terms of spherical polar coordinates as

$$k_{x,inc} = k_0 n_{inc} \sin\theta_{inc} \cos\phi_{inc} \tag{1a}$$

$$k_{y,inc} = k_0 n_{inc} \sin\theta_{inc} \sin\phi_{inc} \tag{1b}$$

$$k_{z,inc} = k_0 n_{inc} \cos\theta_{inc} \tag{1c}$$

where, k_0 is the magnitude of the incident wave vector in vacuum. After diffraction, the different diffracted orders lie on the surface of a cone (as shown in Fig.1) such that all of them have the same y-component, which is also equal to the y-component of the incident wave vector. The x-component of the m^{th} diffracted order changes as per the phase matching diffraction condition $k_{x,m} = k_{x,inc} + mK$, whereas the y-component of the diffracted order remains unchanged from the incident wave ($k_{y,m} = k_{y,inc}$). Thus, $k_{z,m} = \sqrt{k^2 - k_{\rho,m}{}^2}$, where $k_{\rho,m} = \sqrt{k_{x,m}{}^2 + k_{y,m}{}^2}$. Under resonance conditions, the diffracted light (of order m) becomes a guided mode of the waveguide with a propagation constant (β_m) which is equal to the longitudinal component ($k_{\rho,m}$) of the diffracted wave vector $\mathbf{k_m}$. Thus, $\beta_m = \sqrt{k_{x,m}{}^2 + k_{y,m}{}^2}$. Using the expressions of $k_{x,m}$ and $k_{y,m}$ from Equation (1), the propagation constant β_m assumes the form,

$$\beta_m = k_0 \sqrt{(n_{inc} \sin\theta_{inc})^2 + 2 n_{inc} \sin\theta_{inc} \cos\phi_{inc} m \frac{\lambda_0}{\Lambda} + m^2 \frac{\lambda_0{}^2}{\Lambda^2}} \tag{2}$$

This expression is valid for both TE and TM polarizations of the incident light. After diffraction, only certain wavelengths can be guided through the slab waveguide which satisfy the eigenvalue equations of the slab waveguide.[23] Equations S1(a) & (b) in supplementary material (Section I) are the eigenvalue equations for TE and TM polarizations respectively. The parameters of the eigenvalue equations are functions of the propagation constant (β_m) and the refractive indices of various layers. Thus, the resonant wavelengths for the GMR filter at any angle of incidence (θ_{inc}) and azimuthal position (ϕ_{inc}) can be determined by solving the eigenvalue equations by incorporating the expression of β_m given above. Equation (2), therefore provides the basis for the tunable wavelength filter function since the propagation constant of the guided wave depends on the azimuthal angle ϕ_{inc}. Thus, tunable optical filtering can be achieved by azimuthal rotation of the GMR structure. This model shows excellent agreement with our experimental results. In contrast to the model described above, a simpler model which assumes an apparent change in period on azimuthal rotation, shows significant deviation from the experimental data (supplementary material, Section II), thereby showing that this is not the mechanism behind wavelength tuning.

Wavelength tuning was experimentally demonstrated by fabricating a silicon nitride (Si_3N_4, refractive index 2.0) grating and waveguide on a quartz substrate (refractive index 1.45). The grating period was 500 nm with about 50% duty cycle and a depth of 120 nm. The thickness of the waveguide was 80 nm. The fabrication procedure is as follows (Figure S2, supplementary material Section III). 200 nm thick Si_3N_4 was deposited onto a quartz substrate by plasma enhanced chemical vapor deposition (PE-CVD). Next, a positive tone electron beam resist (ZEP-520A-7, Zeon Chemicals) was spin coated to a thickness of 300 nm followed by a charge dissipating agent (ESPACER300, Showa Denko). A 1D grating pattern was then recorded onto the resist surface with electron beam lithography (Table S1, supplementary material Section III). Before development, the substrate was rinsed in de-ionized water to remove the charge dissipating agent. After development, the silicon nitride layer was etched through the electron beam resist mask. Reactive ion etching (RIE) with CF_4 gas (45 sccm, 4 torr, 100W, 1 min) was used for this purpose and an etching depth of 120 nm was achieved. Thus, the grating structure was formed. An un-etched 80 nm layer of Si_3N_4 remained under the grating and served as the waveguide, completing the GMR structure. Finally, a piranha solution

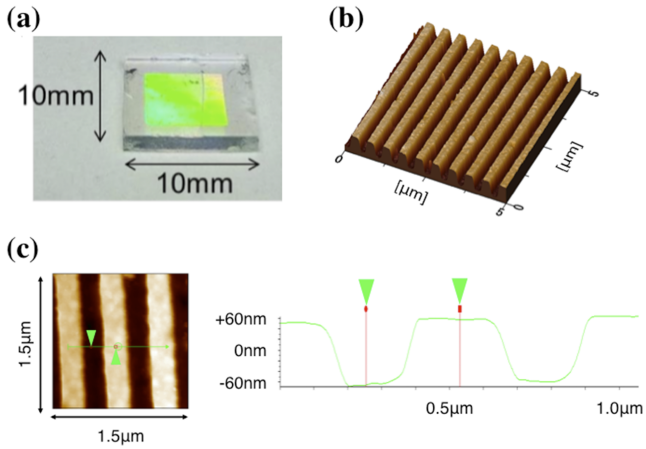

FIG. 2. Characterization of the fabricated GMR structure (a) Photograph of the GMR structure (b) AFM topography of the GMR structure (c) AFM measurements show grating depth to be 120 nm.

(H_2SO_4:H_2O_2= 3:1) was used to remove the residual resist from the substrate. The topography of the GMR structures was measured with an atomic force microscope (AFM) and is provided in Fig. 2. AFM measurements showed that the grating depth and period of the devices were close to the design values. Further, the spectrum obtained from the GMR structure for normal incidence was in excellent agreement with simulated spectrum calculated using the design values (supplementary material Section IV).

Light from a broadband light source was incident on the GMR structure and the scattered light was analyzed with one of two spectrometers depending on the wavelength of the GMR peak (Figure S4, supplementary material Section V). In our experiments the angle of incidence (θ_{inc}) was fixed at 40° and ϕ_{inc} was varied from -90° to +90° in steps of 10° by rotating the GMR structure. The results obtained from the spectrometer are shown in Fig. 3. The GMR peak position was theoretically predicted by solving the eigenvalue equations stated above and showed excellent agreement with the experimental values. Fig. 3(a) shows the location of GMR peaks when the incident light was TE polarized and Fig. 3(b) shows the results when incident light was TM polarized. For each polarization there were two peaks at all azimuthal angles other than ±90° corresponding to the +1 and -1 diffracted orders. The lowest peak wavelength achieved in the experiments was about 470 nm for TM mode without rotation at $\phi = 0°$, whereas the highest peak position was obtained for TE mode at about 1100 nm at $\phi = 90°$. Thus, an extremely wide tuning range of 630 nm was achieved. However, for wavelengths exceeding 875 nm, the reflection efficiency was much lower than that for the lower wavelengths, as shown in Figure 4(a). When the incident light was TM polarized the GMR peak could not be distinguished from background noise for ϕ = -60° to +60°. This may be attributed to

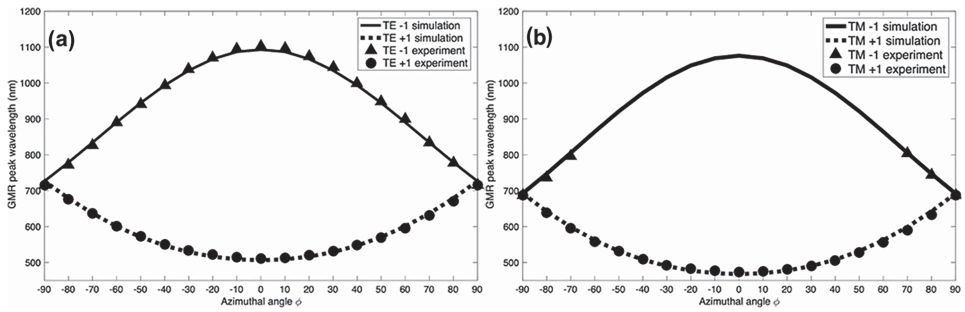

FIG. 3. Wavelength tuning by azimuthal rotation (a) For TE polarization (b) For TM polarization. For both polarizations two peaks corresponding to diffraction orders +1 and -1 are obtained. Thus, the notation TE-1 represents the -1 diffracted order for TE polarization and so on.

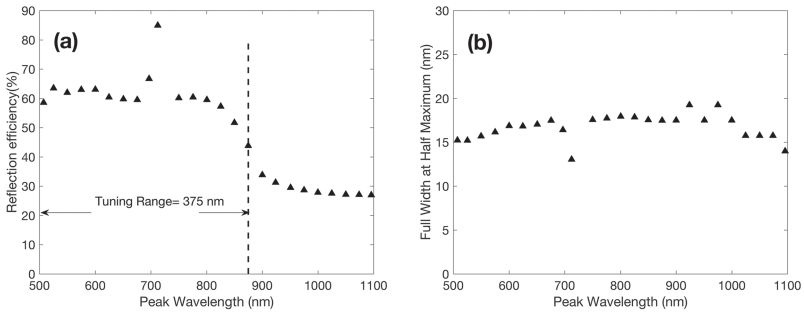

FIG. 4. Efficiency and spectral purity of tunable filter (a) Reflection efficiency, and (b) Full Width at Half Maximum (FWHM) for TE mode.

the fact that out of all the four modes observed in the experiments, the TM-1 mode has the lowest diffraction efficiency.[24] As can be seen from Figure 3 and supplementary material Figure S5, the TE and TM peaks do not overlap. This presents a limitation in filtering unpolarized light. Thus, polarized incident light should be used for practical applications. Figure 3 also shows that at $\phi = \pm 90^{o}$ (fully-conical mounting) the two GMR peak positions merge into one. This is because at $\phi = \pm 90^{o}$, the propagation constants of positive and negative diffraction orders are equal as can be inferred from Equation (2).

Figure 4(a) shows the characteristics of reflection efficiency and spectral purity obtained from the GMR filter for the wavelength range of 500 nm to 1100 nm. The reflection efficiency was typically 60-65% for the visible wavelengths and dropped to about 30% for near infrared (NIR) wavelengths. The mid-point between these two regimes occurs at a wavelength of 875 nm, which was considered as the threshold below which the filter was efficient enough for practical applications. Thus, an extremely wide tuning range of 375 nm was achieved. Notably, even the lowest efficiency value of 27% (at 1100 nm) obtained from our 1D GMR structure is greater than the highest efficiency (<20%) obtained by 2D nanostructures employing azimuthal rotation.[20] The efficiency is especially high at 712 nm (85%), since this wavelength corresponds to fully conical mounting when the peaks of positive and negative diffraction orders merge into one (Figures 3(a) and S5(a)). The GMR peaks exhibit very low reflection at off resonance wavelengths. The full width at half maximum (FWHM) lies within 13 nm~19 nm over the entire range of peak wavelengths, as shown in Figure 4(b).

An apparent color filtering effect produced by rotating the polarization of incident light at normal incidence has been reported previously in GMR structures.[9] Notably, the wavelength tuning by azimuthal rotation as described here is fundamentally different from polarization rotation and the two cases are equivalent only at normal incidence. At oblique incidence, if the azimuthal angle is kept fixed and the polarization is rotated, the propagation constant does not change. Thus, GMR peak positions remain fixed and the effect of rotation is to change the intensity of the peaks relative to each other. Thus, different colors are generated at the output which are additive mixtures of the GMR peak wavelengths (supplementary material Section VI). In contrast, under azimuthal rotation, since the propagation constant is tuned, the GMR peak wavelength itself changes and spectrally pure colors are produced.

In summary, we demonstrated optical tuning over a very wide wavelength range from 500 nm to 875 nm with a single GMR structure. We showed that the resonant wavelength of a 1D GMR structure can be tuned by rotating it about the surface normal, thereby producing a tunable wavelength filter. The proposed method for optical tuning is experimentally simple to realize and does not depend on highly accurate alignment between the sample and the detector as in the case of 2D nanostructures[20] where precise alignment between the cleaved edges of the substrate and the optical fiber is necessary. Moreover, the GMR peak efficiency obtained by our approach (60~65%) is much higher than that from 2D nanostructures (< 20%). Notably, the optical tuning range of 375 nm obtained experimentally with this method is much wider than reported previously for other widely tunable filters.[25] The fabrication parameters of the GMR structure, such as fill fraction and grating depth, can be optimized to achieve higher GMR peak efficiency while retaining the ability to tune over a wide

range of wavelengths. In contrast to the methods requiring out of plane theta rotation and MEMS based tuning mechanisms, the azimuthal rotation approach reported here, is simple to implement using only the GMR structure itself without any additional optical elements. A wide variety of applications are envisaged, for example, hyperspectral imaging as well in astronomical applications requiring tuning over a wide range of wavelengths.[26,27]

SUPPLEMENTARY MATERIAL

See supplementary material for the description of the theoretical model which explains wavelength tuning. They also contain additional details about fabrication and experimental setup.

[1] R. W. Sabnis, Displays **20**, 119 (1999).
[2] Q. Chen, X. Hu, L. Wen, Y. Yu, and D. R. Cumming, Small 1 (2016).
[3] R. Hadar, G. Vincent, S. Collin, N. Bardou, N. Gúrineau, J. Deschamps, and J. L. Pelouard, Appl. Phys. Lett. **96**(22), 3 (2010).
[4] R. Magnusson and S. S. Wang, Appl. Phys. Lett. **61**, 1022 (1992).
[5] D. Wawro, S. Tibuleac, R. Magnusson, and H. Liu, Proc. SPIE **3911**, 86 (2000).
[6] X. Wei and S. M. Weiss, Opt. Express **19**(12), 11330 (2011).
[7] J. H. Schmid, W. Sinclair, J. García, S. Janz, J. Lapointe, D. Poitras, Y. Li, T. Mischki, P. Cheben, A. Delâge, A. Densmore, P. Waldron, and D.-X. Xu, Opt. Express **17**(20), 18371 (2009).
[8] M. J. Uddin and R. Magnusson, Opt. Express **21**(10), 12495 (2013).
[9] M. J. Uddin, T. Khaleque, and R. Magnusson, Opt. Express **22**(10), 12307 (2014).
[10] M. J. Uddin and R. Magnusson, IEEE Photonics Technol. Lett. **24**(17), 1552 (2012).
[11] E.-H. Cho, H.-S. Kim, B.-H. Cheong, O. Prudnikov, W. Xianyua, J.-S. Sohn, D.-J. Ma, H.-Y. Choi, N.-C. Park, and Y.-P. Park, Opt. Express **17**(10), 8621 (2009).
[12] I. Abdulhalim, Chinese Opt. Lett. **7**, 667 (2009).
[13] W. Suh, M. F. Yanik, O. Solgaard, and S. Fan, Appl. Phys. Lett. **82**(13), 1999 (2003).
[14] Y. Kanamori, T. Kitani, and K. Hane, Appl. Phys. Lett. **90**(3), 2007 (2007).
[15] R. Magnusson and Y. Ding, IEEE Photonics Technol. Lett. **18**(14), 1479 (2006).
[16] D. Lacour, G. Granet, J. P. Plumey, and A. M. Ravaud, J. Opt. Soc. Am. A **20**, 1546 (2003).
[17] D. W. Peters, R. R. Boye, and S. A. Kemme, Proc. SPIE **8633**, 86330W (2013).
[18] G. Niederer, W. Nakagawa, H. Peter Herzig, and H. Thiele, Opt. Express **13**, 2196–2200 (2005).
[19] L. Chen, Z. Qiang, H. Yang, H. Pang, Z. Ma, and W. Zhou, Opt. Express **17**, 8396 (2009).
[20] A. Szeghalmi, M. Helgert, R. Brunner, F. Heyroth, U. Gösele, and M. Knez, Adv. Funct. Mater **20**, 2053 (2010).
[21] E. Popov, *Gratings Theory Numeric Applications* (2012), 1.1-1.2.
[22] E. G. Loewen and E. Popov, *Diffraction Gratings and Applications* (CRC Press, New York, 1997), p. 26–27.
[23] S. S. Wang and R. Magnusson, Appl. Opt. **32**(14), 2606 (1993).
[24] M. G. Moharam and T. K. Gaylord, J. Opt. Soc. Am. **73**(4), 451 (1983).
[25] R. Magnusson and M. Shokooh-Saremi, Opt. Express **15**(17), 10903 (2007).
[26] W. Herschel, *Tunable Filters and Large Telescopes* (2001), p. 10.
[27] G. Vincent, E. Sakat, P. Ghenuche, S. Collin, N. Bardou, S. Rommeluère, J. Primot, J. Deschamps, F. Pardo, J.-L. Pelouard, and R. Haïdar, Proc. SPIE **8268**, 826807 (2012).